

# Molecular dynamics simulations of AR+ bombardment of Si with comparison to experiment

**Citation for published version (APA):**

Humbird, D., Graves, D. B., Stevens, A. A. E., & Kessels, W. M. M. (2007). Molecular dynamics simulations of AR+ bombardment of Si with comparison to experiment. *Journal of Vacuum Science and Technology A*, 25(6), 1529-1533. <https://doi.org/10.1116/1.2787713>

**DOI:**

[10.1116/1.2787713](https://doi.org/10.1116/1.2787713)

**Document status and date:**

Published: 01/01/2007

**Document Version:**

Publisher's PDF, also known as Version of Record (includes final page, issue and volume numbers)

**Please check the document version of this publication:**

- A submitted manuscript is the version of the article upon submission and before peer-review. There can be important differences between the submitted version and the official published version of record. People interested in the research are advised to contact the author for the final version of the publication, or visit the DOI to the publisher's website.
- The final author version and the galley proof are versions of the publication after peer review.
- The final published version features the final layout of the paper including the volume, issue and page numbers.

[Link to publication](#)

**General rights**

Copyright and moral rights for the publications made accessible in the public portal are retained by the authors and/or other copyright owners and it is a condition of accessing publications that users recognise and abide by the legal requirements associated with these rights.

- Users may download and print one copy of any publication from the public portal for the purpose of private study or research.
- You may not further distribute the material or use it for any profit-making activity or commercial gain
- You may freely distribute the URL identifying the publication in the public portal.

If the publication is distributed under the terms of Article 25fa of the Dutch Copyright Act, indicated by the "Taverne" license above, please follow below link for the End User Agreement:

[www.tue.nl/taverne](http://www.tue.nl/taverne)

**Take down policy**

If you believe that this document breaches copyright please contact us at:

[openaccess@tue.nl](mailto:openaccess@tue.nl)

providing details and we will investigate your claim.

# Molecular dynamics simulations of Ar<sup>+</sup> bombardment of Si with comparison to experiment

David Humbird<sup>a)</sup>

Lam Research Corporation, 4400 Cushing Parkway, Fremont, California 94538

David B. Graves

Department of Chemical Engineering, University of California, Berkeley, California 94720

A. A. E. Stevens and W. M. M. Kessels

Department of Applied Physics, Eindhoven University of Technology, P.O. Box 513, 5600 MB Eindhoven, The Netherlands

(Received 3 July 2007; accepted 28 August 2007; published 26 September 2007)

The authors present molecular dynamics (MD) simulations of energetic Ar<sup>+</sup> ions (20–200 eV) interacting with initially crystalline silicon, with quantitative comparison to experiment. Ar<sup>+</sup> bombardment creates a damaged or amorphous region at the surface, which reaches a steady-state thickness that is a function of the impacting ion energy. Real-time spectroscopic ellipsometry data of the same phenomenon match the MD simulation well, as do analogous SRIM simulations. They define positional order parameters that detect a sharp interface between the amorphous and crystalline regions. They discuss the formation of this interesting feature in the simulation, and show that it provides insight into some assumptions made in the analysis of experimental data obtained by interface-sensitive surface spectroscopy techniques. © 2007 American Vacuum Society. [DOI: 10.1116/1.2787713]

## I. INTRODUCTION

Nonequilibrium plasma discharges are widely used in industrial material processing operations, including integrated circuit manufacture, thin film transistor flat panel display manufacture, microelectromechanical systems manufacture, and associated industries. Molecular gases introduced into nonequilibrium plasmas dissociate and generally become weakly ionized. Positive ions from the plasma impact surfaces with energies from several electron volts to several kiloelectron volts of kinetic energy. The effects of such energetic species bombarding Si surfaces have been studied with beam experiments<sup>1–3</sup> as well as atomistic simulation techniques.<sup>4–8</sup>

Molecular dynamics (MD) is a particularly useful computational technique for simulating ion impacts on surfaces. A low- to medium-energy ion impact (kinetic energy <1 keV) on a surface can be expected to last for no more than a few picoseconds, and its collision cascade is confined to the volume occupied by no more than a few thousand atoms. These time and length scales happen to be commensurate with those that are readily tractable using MD on a standard desktop computer. A strength of MD is that impact trajectories can be examined individually, providing atomic-scale detail of the fundamental plasma-surface interactions at work. The accuracy of such details, however, is only as good as the quantitative agreement between the simulation and well-defined experiments. As better agreement is shown, the simulation details can be assumed to be more reliable.

Few such direct comparisons of simulation and experiment exist in the MD literature today; this is a goal of the

present article. Here, we present MD simulations of energetic Ar<sup>+</sup> impacts on initially crystalline silicon, and make comparisons to experimental results from a multiple-beam system for studying Si etching at the Eindhoven University of Technology.<sup>3,9–11</sup> In this multiple-beam study, the interaction of low-energy ions (70–2000 eV) with crystalline silicon has recently been studied by spectroscopic ellipsometry and optical second harmonic generation.<sup>3,12</sup> We find reasonable quantitative agreement between the experimental measurements and directed simulations of the same phenomena. The details ascertained from the simulation also justify some of the assumptions made in the experiments. The simulations presented here were newly performed using the Tersoff Si potential.<sup>13</sup> We observe behavior that is qualitatively similar to previous calculations<sup>14</sup> using the potential of Stillinger and Weber,<sup>15</sup> but with quantitative differences.

## II. DESCRIPTION OF THE SIMULATION

Molecular dynamics refers to a class of simulations that solve Newton's equations of motion for a system of interacting particles. The repulsive and attractive interactions between atoms are modeled by interatomic potential energy functions. The system's potential energy surface is given by analyzing all unique atomic interactions in the system. The negative gradient of the potential energy surface with respect to an atom's position yields the three-dimensional force acting on that atom. Given this force, and the assumption that atoms behave as classical particles, Newton's equations of motion may be integrated numerically to compute the atom's trajectory.<sup>16</sup> Further details of MD simulation techniques can be found in Ref. 17.

<sup>a)</sup>Electronic mail: dave.humbird@lamrc.com

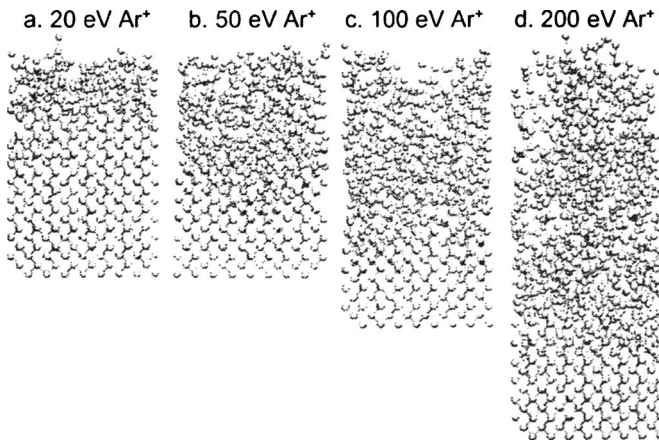


FIG. 1. Snapshot images of simulation cells after 30 ML of Ar<sup>+</sup> ion bombardment at 20–200 eV. The material was initially crystalline silicon.

Impacts of Ar<sup>+</sup> on initially crystalline silicon were previously considered with MD simulations<sup>14</sup> using the Stillinger-Weber interatomic potential for Si.<sup>15</sup> The present results used the Si potential of Tersoff.<sup>13</sup> In either case, a repulsive Molière pair potential was used for all argon interactions.<sup>18</sup> The simulations began with a cell of silicon atoms with an exposed area of 470 Å<sup>2</sup>. Periodic boundaries were imposed in the lateral dimensions and the bottom layer of atoms was held fixed. The initial surface used was (100) crystalline, 2 × 1 reconstructed, at room temperature. At the beginning of each impact, the incident Ar was introduced at a random location above the surface and given a prescribed kinetic energy. The Ar was directed to the surface at normal incidence unless noted otherwise. For each impact trajectory, the motion of all atoms was followed for 0.5 ps. A heat bath was applied between impacts to allow the cell to return to 300 K.<sup>19</sup> Events occurring between impacts were not simulated; it was assumed that nothing happens in this interval except cooling of the surface to 300 K and desorption of any weakly bound Si atoms or clusters and rare gas atoms, which were removed by the code as described elsewhere.<sup>20</sup> Coverages and fluences are reported in units of monolayer (ML), with 1 ML corresponding to  $\sim 7 \times 10^{14}$  atoms cm<sup>-2</sup>. Although “ion” refers to energetic species, in fact, it is assumed that ions are neutralized just before impact and are interacting with the surface as neutrals.<sup>21</sup>

### III. RESULTS AND DISCUSSION

#### A. The steady-state amorphous layer

As energetic Ar<sup>+</sup> ions strike an initially crystalline Si surface, the top atoms are pushed aside in the collision cascade, creating a damaged or amorphous layer. Figure 1 shows the amorphous layers resulting from 30 ML of Ar<sup>+</sup> fluence at a range of energies from 20 to 200 eV. Below the amorphous layer, the silicon atoms remain crystalline with a rather sharp interface between. The depth of this interface below the top-most atoms is how we define the amorphous layer thickness.

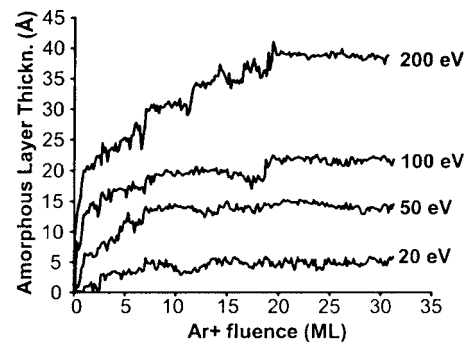


FIG. 2. Evolution of the amorphous layer thickness as a function of ion fluence for Ar<sup>+</sup> ion energies from 20 to 200 eV. Onset of damage is rapid, with a slower approach to steady state.

We used an order parameter to quantitatively define the location of the interface. The interface and the order parameter will be discussed in greater detail later.

At higher fluence, the amorphous layer reaches a steady-state thickness. Figure 2 shows how the amorphous layer thickness increases with ion fluence in the simulation, with Ar<sup>+</sup> impacts in the range of 20–200 eV. There is a rapid onset of damage, with the amorphous layer thickness reaching 50% of its steady-state value in the first monolayer of ion fluence. This is followed by a slower approach to steady state. With all ion energies studied here, the steady-state thickness is reached within 20 total monolayers of fluence. Further impacts induce noise in the measured thickness, but do not change it significantly.

Figure 3 compares another set of simulation results to analogous experimental data. In the experiment, an initially crystalline Si sample was bombarded with Ar<sup>+</sup> ions at 70 eV and 45° incidence. The sample was monitored *in situ* by spectroscopic ellipsometry (SE). The SE data were used to determine the thickness of the damaged layer in real time as it was induced by the ion bombardment.<sup>3,22</sup> An analogous simulation was performed at the same ion energy and incident angle. We see that the experimental data match the simulation data rather well, both in the magnitude and the time (or fluence) scale of ion damage.

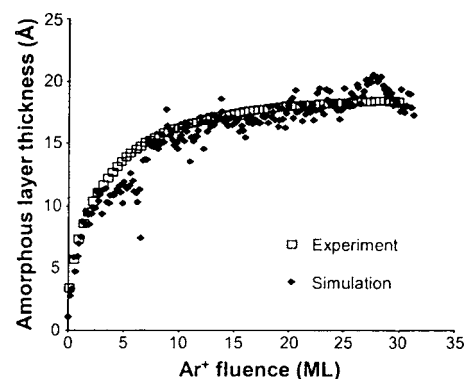


FIG. 3. Evolution of the amorphous layer thickness: MD simulation vs real-time spectroscopic ellipsometry experiment. In both the experiment and simulation, the Ar<sup>+</sup> ion energy is 70 eV and the angle of incidence is 45°.

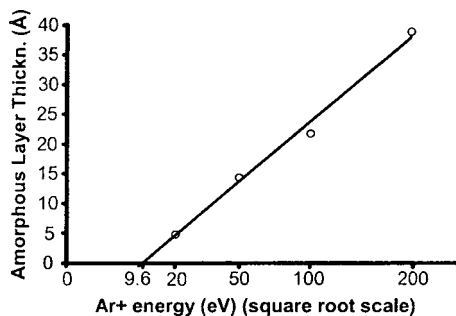


FIG. 4. Square-root dependence of the amorphous layer thickness on ion energy. Below 9.6 eV, ions do not damage the surface significantly.

As mentioned above, the thickness of the amorphous layer at steady state is a function of the impacting ion energy. Figure 4 displays the steady-state thickness from the simulations for the energy range of 20–200 eV. The steady-state amorphous thickness has a linear relationship with the square root of the ion energy. Such  $E^{1/2}$  relationships have been observed previously by molecular dynamics<sup>23</sup> and also experimentally, for instance, in the sputtering experiments reported by Steinbrüchel.<sup>24</sup> The line in Fig. 4 does not pass through the origin. Instead, when extrapolated to zero amorphous layer thickness, we obtain an ion energy of 9.6 eV. This energy may be thought of as a threshold below which Si atoms are not displaced with a high probability, so the surface sustains no damage.<sup>24</sup> The observed value of 9.6 eV is expected to be a function of the ion mass, incident angle, and perhaps also the crystalline orientation.<sup>24,25</sup>

Further agreement between simulation and experiment is shown in Fig. 5. The amorphous layer thickness as a function of ion energy is compared for the spectroscopic ellipsometry data and SRIM (the stopping and range of ions in matter) simulations of Stevens *et al.*,<sup>3</sup> and the molecular dynamics simulations of this work and the previous paper of Humbird and Graves.<sup>14</sup> In the SRIM simulations, the creation of vacancies is chosen to be the measure for permanent damage of

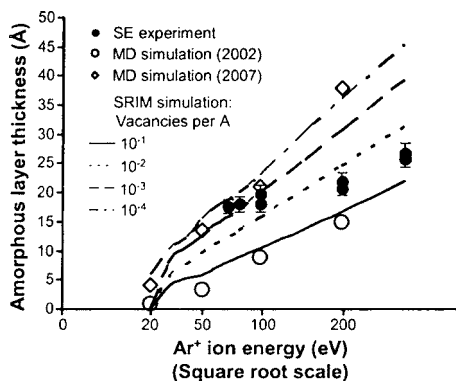


FIG. 5. Amorphous layer thickness as measured by ellipsometry, and predicted by MD and SRIM simulations. In the SRIM simulations, the creation of vacancies is chosen to be the measure for permanent damage of the crystalline silicon, data is given for different vacancy levels. MD simulation (2002) refers to the results of Ref. 14, and MD simulation (2007) represents the results of this article.

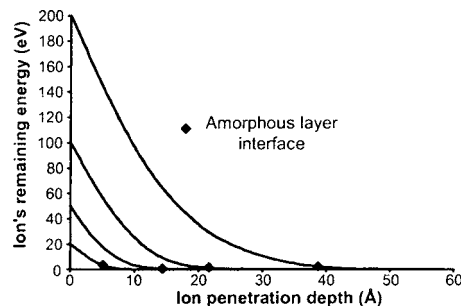


FIG. 6. Characterization of an ion's remaining energy as it descends into a Si surface for a range of energies. In each case, the depth of the amorphous-crystalline interface is marked with a diamond.

the crystalline silicon and results are shown for vacancy levels of  $10^{-1}$ ,  $10^{-2}$ ,  $10^{-3}$ , and  $10^{-4}$  vacancy/Å averaged over  $10^6$  single ion impacts at  $45^\circ$  incidence.<sup>3</sup> Again the data are plotted in Fig. 5 with ion energy represented on the square-root scale, since this is the expected dependence. The amorphous layer thickness increases essentially linearly with  $E^{1/2}$  for each computational technique. The linear dependence is less clear with the SE experimental data of Stevens *et al.*, but their measurements do fall between the different simulation data sets. Above 100 eV, the SE measurements clearly follow the  $E^{1/2}$  shape.

## B. The amorphous-crystalline interface

As discussed above, the silicon below the amorphous layer remains crystalline, and a rather sharp interface is found between the two layers. In Fig. 6, we have characterized the ions remaining energy as they descend into the amorphized surface. This calculation was performed by averaging over several thousand impacts on each of the simulation cells displayed in Fig. 1. The depth of the amorphous-crystalline interface is marked on each curve in Fig. 6 with a diamond, and in each case, it falls near zero remaining ion energy. We note that in the previous simulations of Humbird and Graves,<sup>14</sup> the amorphous-crystalline interface occurred at considerably higher ion energy, between 10 and 12 eV remaining. This is a function of the interatomic potential used; in the previous simulations, the Stillinger-Weber potential used had a longer cutoff radius, which effectively created a stiffer material than the Tersoff potential used here. The matter of which potential is “correct” is, of course, open for debate; however, the Tersoff Si potential and its derivatives have shown better agreement with experiment, here and elsewhere,<sup>26,27</sup> so we may therefore assert that the Tersoff potential is the more accurate one. In any event, the qualitative result is robust: the amorphous-crystalline interface is sharp and is located at roughly the ion stopping length.

We now turn to the discussion of order in the amorphous and crystalline phases. In order to quantitatively determine the location of the interface, we defined a positional order parameter,



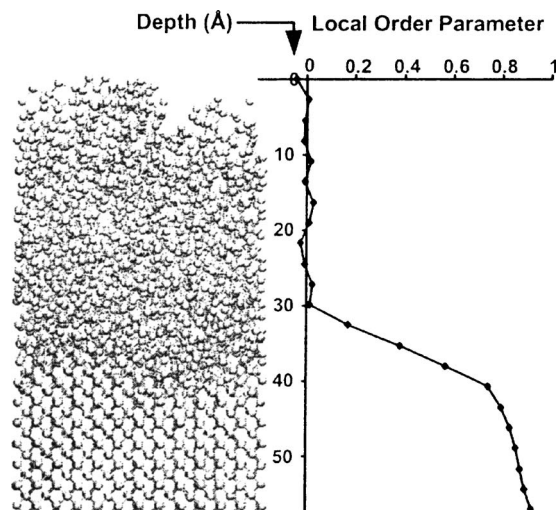


FIG. 7. Order in the simulation cell as a function of depth. A local order parameter  $\xi=0$  means amorphous, and  $\xi=1$  means ideally crystalline. The interface is locally sharp but varies in height across the cell.

$$\xi = \frac{1}{3}(\lambda_x + \lambda_y + \lambda_z), \quad (1)$$

with

$$\lambda_x = \frac{1}{N_{\text{atom } i}} \sum_{i=1}^N \cos\left(\frac{8\pi}{a}x_i\right), \quad (2)$$

where  $x_i$  is the  $x$  position of atom  $i$  in the lattice and  $a$  is the lattice constant. This function switches smoothly from 1 to 0 as atoms leave their sites in the diamond cubic lattice (i.e., positions at integer multiples of  $a/4$ ). When averaged, this order parameter therefore resolves to zero for a liquid or amorphous solid and unity for a perfectly crystalline material. In practice, the order parameter in a vibrating, crystalline simulation cell is actually slightly less than unity due to finite size limitations. This is a simple approach, but demonstrates the following point capably.

This order parameter can be expressed as a function of depth ( $z$ ) by dividing the simulation cell into discrete zones of  $a/2$  (about 2.7 Å) and computing  $\xi$  for the  $N_z$  atoms in each zone. The resulting data were smoothed by also including the atoms in the zones immediately above and below. In the results presented above, the amorphous-crystalline interface was defined to be the depth at which the positional order parameter was equal to 0.15. This threshold value was chosen to be slightly larger than the uncertainty in the computation, which is on the order of  $\pm 0.1$ . As will be shown in Fig. 7, the threshold value of 0.15 captures the interface location fairly accurately.

Figure 7 displays the order parameter computed for a representative simulation cell as a function of depth. This cell was amorphized with 200 eV Ar<sup>+</sup>. For better atomic statistics, we used a cell with twice the lateral dimensions of the cells in Fig. 1. The depth scale for the right-hand plot corresponds directly to the snapshot on the left. For the cell shown here, the order parameter clearly discerns between the amorphous region in the top 30 Å ( $\xi=0$ ) and the crystalline re-

gion ( $\xi \sim 1$ ) below. The interface between these two regions is rather sharp; however, the depth plot shows a transitional region of about 10 Å; this transition arises because although the interface is locally sharp, it is not uniformly flat. This can be seen in the snapshot: the interface is perceptibly higher on the left side.

This sharp interface has implications for experimental spectroscopic techniques that can be used to study the interaction of ion and radical beams with crystalline silicon. For example, data obtained by *in situ* SE, used here for determining the thickness of the amorphized layer due to Ar<sup>+</sup> impact,<sup>3,11</sup> relies on optical-model-based analysis. In such a model, the sample is described by one or more thin layers stacked on a semi-infinite substrate. Each of the layers has distinct optical properties yielding contrast to distinguish between them in the data analysis provided that the interfaces are sufficiently sharp. Optical secondary harmonic generation (SHG) is another technique that recently has been employed to study the interaction of Ar<sup>+</sup> with crystalline silicon.<sup>12</sup> SHG is a nonlinear optical technique that is highly surface and interface sensitive and, therefore, powerful to study the interaction of ion and radical beams with a surface. It has been demonstrated that the interpretation of the data obtained by SHG also requires a multilayer optical model. In the data analysis, a sharp interface between amorphous and crystalline silicon was found to be an important assumption.<sup>12</sup> The MD simulations presented here justify this assumption.

#### IV. CONCLUDING REMARKS

We have shown with molecular dynamics simulations that energetic Ar<sup>+</sup> bombardment of crystalline Si creates a damaged or amorphous region at the surface, with crystalline material remaining beneath. At sufficiently high ion fluence ( $>20$  monolayers), the amorphous layer reaches a steady-state thickness that is a function of the impacting ion energy. Spectroscopic ellipsometry data collected during a beam experiment of the same phenomenon were shown to match the MD simulation well, both in the magnitude and the time scale of ion damage. It was further shown that the MD simulations, analogous SRIM simulations, and the beam experiments were all in generally good quantitative agreement, within their respective assumptions.

We further demonstrated that the interface between the amorphous and crystalline layers is rather sharp and is located at roughly the ion stopping length. We defined positional order parameters to quantitatively describe order in the different layers as a function of subsurface depth and found that these parameters are able to clearly distinguish the amorphous region from the crystalline region. The sharp interface detected by the simulations justifies some assumptions that are routinely made in spectroscopic techniques such as ellipsometry and second harmonic generation. Both these techniques involve the analysis of raw spectra by modeling the optical response in a multiple-layer approach describing different materials, assuming the interface between layers is sharp.

## ACKNOWLEDGMENTS

The work of one of the authors (W.M.M.K.) has been made possible by the fellowship of the Royal Netherlands Academy of Arts and Sciences (KNAW). The KNAW is also acknowledged for financially supporting a sabbatical leave at UC Berkeley.

- <sup>1</sup>H. F. Winters and J. W. Coburn, *Surf. Sci. Rep.* **14**, 161 (1992) and references therein.
- <sup>2</sup>J. P. Chang and H. H. Sawin, *J. Vac. Sci. Technol. A* **15**, 610 (1997).
- <sup>3</sup>A. A. E. Stevens, W. M. M. Kessels, M. C. M. van de Sander, and H. C. W. Beijerinck, *J. Vac. Sci. Technol. A* **24**, 1933 (2006).
- <sup>4</sup>D. B. Graves and D. Humbird, *Appl. Surf. Sci.* **192**, 72 (2002).
- <sup>5</sup>D. Humbird and D. B. Graves, *J. Vac. Sci. Technol. A* **23**, 31 (2005).
- <sup>6</sup>J. F. Ziegler, J. P. Biersack, and U. Littmark, *The Stopping Range of Ions in Solids* (Pergamon, Oxford, 1985).
- <sup>7</sup>T. A. Schoolcraft, in *23rd International Symposium on Dry Process Conference Proceedings* (The Institute of Electrical Engineers of Japan, Tokyo, Japan, 2001), pp. 29–36, and references therein.
- <sup>8</sup>L. Hanley and S. B. Sinnott, *Surf. Sci.* **500**, 500 (2002).
- <sup>9</sup>G. J. P. Joosten, M. J. M. Vugts, H. J. Spruijt, H. A. J. Senhorst, and H. C. W. Beijerinck, *J. Vac. Sci. Technol. A* **12**, 636 (1994).
- <sup>10</sup>M. J. M. Vugts, G. J. P. Joosten, A. van Oosterum, H. A. J. Senhorst, and H. C. W. Beijerinck, *J. Vac. Sci. Technol. A* **12**, 2999 (1994).
- <sup>11</sup>A. A. E. Stevens and H. C. W. Beijerinck, *J. Vac. Sci. Technol. A* **23**, 134 (2005).
- <sup>12</sup>J. J. H. Gielis, P. M. Gevers, A. A. E. Stevens, H. C. W. Beijerinck, M. C. M. van de Sanden, and W. M. M. Kessels, *Phys. Rev. B* **74**, 165311 (2006).
- <sup>13</sup>J. Tersoff, *Phys. Rev. B* **38**, 9902 (1988).
- <sup>14</sup>D. Humbird and D. B. Graves, *Pure Appl. Chem.* **74**, 419 (2002).
- <sup>15</sup>F. H. Stillinger and T. A. Weber, *Phys. Rev. B* **31**, 5262 (1985).
- <sup>16</sup>W. C. Swope, H. C. Andersen, P. H. Beren, and K. R. Wilson, *J. Chem. Phys.* **76**, 637 (1982).
- <sup>17</sup>J. M. Haile, *Molecular Dynamics Simulation* (Wiley, New York, 1992).
- <sup>18</sup>I. Torrens, *Interatomic Potentials* (Academic, New York, 1972).
- <sup>19</sup>H. J. C. Berendsen, J. P. M. Postma, W. F. van Gunsteren, A. DiNola, and J. R. Haak, *J. Chem. Phys.* **81**, 3684 (1984).
- <sup>20</sup>D. Humbird and D. B. Graves, *J. Appl. Phys.* **96**, 791 (2004).
- <sup>21</sup>H. D. Hagstrum, *Phys. Rev.* **122**, 83 (1960).
- <sup>22</sup>From the ellipsometry data it cannot be distinguished whether the thickness of the amorphous layer increases or whether the amorphous fraction of the layer increases with time/fluence. For simplicity we refer to “an increasing thickness over time/fluence.”
- <sup>23</sup>M. E. Barone and D. B. Graves, *J. Appl. Phys.* **77**, 1263 (1995).
- <sup>24</sup>C. Steinbrüchel, *Appl. Phys. Lett.* **55**, 1960 (1989).
- <sup>25</sup>W. Eckstein, C. García-Rosales, J. Roth, and J. László, *Nucl. Instrum. Methods Phys. Res. B* **83**, 95 (1993).
- <sup>26</sup>D. Humbird and D. B. Graves, *Plasma Sources Sci. Technol.* **13**, 548 (2004).
- <sup>27</sup>D. Humbird and D. B. Graves, *J. Chem. Phys.* **120**, 2405 (2004).